

# Numerical simulation of a 2D squirmer in a rectangular microchannel

Harshita Tiwari and Sanket Biswas

(GCT/1940097 and GCT/1940108)

under the supervision of

Dr. Kamlesh Kumari

Department of Chemical Engineering  
SLIET Longowal

and the joint external supervision of

Dr. Shubhadeep Mandal and Dr. Aloke Kumar

Department of Mechanical Engineering  
IISc Bengaluru

May 19, 2023



# Contents

- 1 Introduction
- 2 Swimming dynamics in unbounded quiescent fluid
  - Mathematical modelling
  - Numerical method
  - Results and discussion
- 3 Swimming dynamics in confined quiescent fluid
  - Mathematical modelling
  - Numerical method
  - Results and discussion



# Introduction

## Background & Motivation

- *Microswimmers* show active motion and convert free energy from their environment into persistent motion.
- The *squirm model* has been widely used to explore the swimming dynamics of microswimmers in various fluid environments for the last five or six decades.
- Past studies have revealed intriguing variations in the locomotion of squirmers when confined in spaces of various sizes or in proximity to smooth/rough boundaries, due to hydrodynamic and non-hydrodynamic interactions.
- The squirm model has proved to be extremely accurate for studying the near-field swimming behaviour of swimmers, such as its behaviour near a wall or another *active* or *passive particle*.
- While researchers have explored numerical simulation using the *lattice Boltzmann method (LBM)*, using the *finite element method (FEM)* in simulation software has been less explored.
- Numerical simulation of swimmers in complex-confined fluidic domains offers cost-effective, controlled, and detailed investigations into their behavior, allowing for designing various control and navigation strategies.
- The study of microswimmer dynamics has promising applications in various fields, such as sperm locomotion, artificial micro-bot formation, biofilm formation, drug delivery, mixing, and sensing.



# Overview of our research

## Progress so far

- ① Conducted a thorough literature review to identify and define the problem statement.
- ② Improved the numerical model of Ahana and Thampi [1] using the finite element method (FEM).
- ③ Developed the corresponding governing equations of motion (EOMs) of a microswimmer, using the squirmer model proposed by Lighthill [2], Blake [3], in both unbounded and confined domains with quiescent fluid.
- ④ Designed a self-sustainable numerical simulation framework for CFD softwares such as COMSOL and OpenFOAM.

## Possible future work

- ① Extending our numerical simulation framework to include non-inertial microswimmers in confined domains with plane and oscillatory Poiseuille flow.
- ② Further extending our numerical simulation framework to include microswimmer inertia.



# Mapping of COs and POs

Our project maps the program objectives (POs) and course objectives (COs) as follows:

POs & COs	PO1	PO2	PO3	PO4	PO5	PO6	PO7	PO8	PO9	PO10	PO11	PO12	PSO1	PSO2
CO1	S	S	W	S	S	M	S	S	S	S	M	M	M	S
CO2	S	S	S	S	S	S	M	S	S	S	M	M	M	S
CO3	S	M	M	S	S	M	S	S	S	S	M	M	M	S



# Contents

- 1 Introduction
- 2 Swimming dynamics in unbounded quiescent fluid
  - Mathematical modelling
  - Numerical method
  - Results and discussion
- 3 Swimming dynamics in confined quiescent fluid
  - Mathematical modelling
  - Numerical method
  - Results and discussion



# Squirmer model

- We employed the *squirmer model* proposed by Lighthill [2] and Blake [3].
- A squirmer is defined as a circular rigid particle having a prescribed *surface slip velocity*

$$\mathbf{u}^S(x_s) = \sum_{n=0}^{\infty} A_n \cos(n\theta) \hat{\mathbf{e}}_r + \sum_{n=0}^{\infty} B_n \sin(n\theta) \hat{\mathbf{e}}_\theta. \quad (1)$$

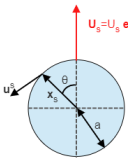


Figure: Schematic diagram illustrating a squirmer of radius  $a$ .

- We employed a simplified squirmer model:

$$\mathbf{u}^S(x_s) = \sum_{n=0}^2 B_n \sin(n\theta) \hat{\mathbf{e}}_\theta = (B_1 \sin \theta + 2B_2 \sin \theta \cos \theta) \hat{\mathbf{e}}_\theta. \quad (2)$$

- The squirmer develops a flow field,  $\mathbf{u} = u_r \hat{\mathbf{e}}_r + u_\theta \hat{\mathbf{e}}_\theta$ :

$$u_r(r, \theta) = \frac{B_1}{2} \left( \frac{a}{r} \right)^2 \cos \theta + \sum_{n=2}^{\infty} \frac{n}{2} B_n \cos(n\theta) \frac{a^{n-1}}{r^{n-1}} \left[ \left( \frac{a}{r} \right)^2 - 1 \right], \quad (3a)$$

$$u_\theta(r, \theta) = \frac{B_1}{2} \left( \frac{a}{r} \right)^2 \sin \theta + \sum_{n=2}^{\infty} \frac{1}{2} B_n \sin(n\theta) \frac{a^{n-1}}{r^{n-1}} \left[ n \left( \frac{a}{r} \right)^2 - (n-2) \right]. \quad (3b)$$

# Types of squirmers

- In an unbounded fluid, a squirmer translates with a velocity

$$\mathbf{U}_s = U_s \hat{\mathbf{e}} = \mathbf{u}(r = a, \theta = 0) = \frac{B_1}{2} \hat{\mathbf{e}}_r. \quad (4)$$

- The  $B_1$  mode determines the translational velocity, and the coefficient  $B_2$  describes the intensity of vorticity.
- The next modes are characterized by

$$\beta_n = \frac{B_n}{B_1}, \quad n \in \mathbb{Z}_{\geq 2}. \quad (5)$$

- $\beta_2 = B_2/B_1$ , the *squirmer self-propulsion strength*, represents three types of squirmers: *pushers* ( $\beta < 0$ ), *pullers* ( $\beta > 0$ ), and *neutral squirmers* ( $\beta = 0$ ).
- Pushers: *E. coli* and *B. subtilis*; pullers: *C. reinhardtii* and *Euglena gracilis*; neutral squirmers like *Volvox carteri* and *Tetrahymena thermophila*.

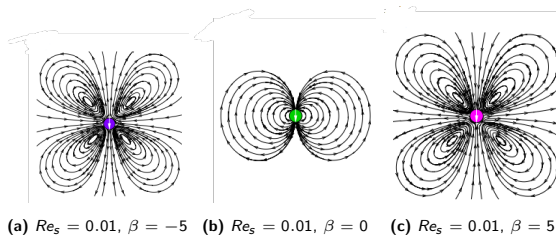


Figure: Illustration of streamlines around squirmers with different propulsion strengths  $\beta$ .

# Domain specifications in co-moving frame

- Squirmer of radius  $a$ , initially positioned at  $x_0 = (x_0, y_0)$ .
- Unbounded quiescent fluid: density  $\rho$ , dynamic viscosity  $\mu$ , Reynolds number:

$$Re_s = \frac{\rho U_s a}{\mu} = \frac{\rho B_1 a}{2\mu}. \quad (6)$$

- The fluid dynamics around the squirmer is governed by the incompressible Navier-Stokes equations:

$$\nabla \cdot \mathbf{u} = 0, \quad (7a)$$

$$\rho \left( \frac{\partial \mathbf{u}}{\partial t} + \mathbf{u} \cdot \nabla \mathbf{u} \right) = -\nabla p + \mu \nabla^2 \mathbf{u}, \quad (7b)$$

$\mathbf{u}$  and  $p$  represent the velocity and pressure fields, respectively. Eqn. (7) is solved using FEM in COMSOL.

- *Co-moving frame*: A frame that translates along with the squirmer.

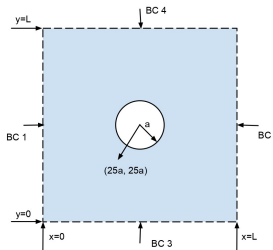


**Figure:** The figure illustrates the initial setup of an unbounded fluid medium in the co-moving frame, represented by a square domain with a side length of  $L = 50a$ , containing a two-dimensional disk squirmer of radius  $a$  initially positioned at  $x_0 = (25a, 25a)$ . The fluid velocity satisfies the initial and boundary conditions given in Eqn. (9).

# Initial and boundary conditions in co-moving frame

- Lab frame initial and boundary conditions:

$$\text{IC 1: } \mathbf{u}(x, y, t) = \mathbf{0} \text{ at } 0 \leq x \leq L, 0 \leq y \leq L, t = 0, \quad (8a)$$

$$\text{BC 1: } \mathbf{u}(x, y, t) = \mathbf{0} \text{ at } x = 0, 0 \leq y \leq L, t \geq 0, \quad (8b)$$

$$\text{BC 2: } \mathbf{u}(x, y, t) = \mathbf{0} \text{ at } x = L, 0 \leq y \leq L, t \geq 0, \quad (8c)$$

$$\text{BC 3: } \mathbf{u}(x, y, t) = \mathbf{0} \text{ at } 0 \leq x \leq L, y = 0, t \geq 0, \quad (8d)$$

$$\text{BC 4: } \mathbf{u}(x, y, t) = \mathbf{0} \text{ at } 0 \leq x \leq L, y = L, t \geq 0. \quad (8e)$$

(8)

- Co-moving frame initial and boundary conditions:

$$\text{IC 1: } \mathbf{u}(x, y, t) = -\mathbf{U}_s(t = 0) \text{ at } 0 \leq x \leq L, 0 \leq y \leq L, t = 0, \quad (9a)$$

$$\text{BC 1: } \mathbf{u}(x, y, t) = -\mathbf{U}_s(t) \text{ at } x = 0, 0 \leq y \leq L, t \geq 0, \quad (9b)$$

$$\text{BC 2: } \mathbf{u}(x, y, t) = -\mathbf{U}_s(t) \text{ at } x = L, 0 \leq y \leq L, t \geq 0, \quad (9c)$$

$$\text{BC 3: } \mathbf{u}(x, y, t) = -\mathbf{U}_s(t) \text{ at } 0 \leq x \leq L, y = 0, t \geq 0, \quad (9d)$$

$$\text{BC 4: } \mathbf{u}(x, y, t) = -\mathbf{U}_s(t) \text{ at } 0 \leq x \leq L, y = L, t \geq 0, \quad (9e)$$

(9)

$\mathbf{U}_s(t)$ : velocity of the squirmer at time  $t$ .

- Note: There's no change in the fluid dynamics around the squirmer due to the frame change.



# Squirmer dynamics: surface velocity

- Squirmer's position:  $\mathbf{x} = x\hat{\mathbf{e}}_x + y\hat{\mathbf{e}}_y$ ; orientation:  $\hat{\mathbf{e}} = e_x\hat{\mathbf{e}}_x + e_y\hat{\mathbf{e}}_y$ ; translational velocity:  $\mathbf{U}_s = U_s\hat{\mathbf{e}} = U_x\hat{\mathbf{e}}_x + U_y\hat{\mathbf{e}}_y$ ; rotational velocity:  $\boldsymbol{\Omega} = \Omega\hat{\mathbf{e}}_z$ .

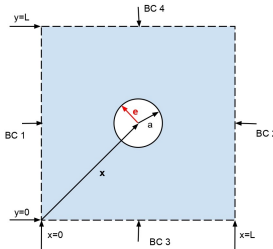


Figure: Schematic representation of the position and orientation of the squirmer in an unbounded quiescent fluid.

- In the lab frame:

$$\begin{aligned}\mathbf{u}_s(\mathbf{x}_s) &= \mathbf{u}^S(\mathbf{x}_s) + \mathbf{U}_s + \boldsymbol{\Omega} \times \mathbf{x}_s \\ &= B_1 (\sin \theta + 2\beta \sin \theta \cos \theta) \hat{\mathbf{e}}_\theta + \mathbf{U}_s + \boldsymbol{\Omega} \times \mathbf{x}_s.\end{aligned}\tag{10}$$

- In the co-moving frame:

$$\begin{aligned}\mathbf{u}_s(\mathbf{x}_s) &= \mathbf{u}^S(\mathbf{x}_s) + \boldsymbol{\Omega} \times \mathbf{x}_s \\ &= B_1 (\sin \theta + 2\beta \sin \theta \cos \theta) \hat{\mathbf{e}}_\theta + \boldsymbol{\Omega} \times \mathbf{x}_s.\end{aligned}$$



# Squirmer dynamics: governing EOMs

- Component-wise governing EOMs in the lab frame:

$$\frac{dx}{dt} = U_x, \quad \frac{dy}{dt} = U_y, \quad (12a)$$

$$\frac{de_x}{dt} = -\Omega e_y, \quad \frac{de_y}{dt} = \Omega e_x, \quad (12b)$$

$$\frac{dU_x}{dt} = \frac{1}{m} \iint_A f_x(x_s) dA, \quad (12c)$$

$$\frac{dU_y}{dt} = \frac{1}{m} \iint_A f_y(x_s) dA, \quad (12d)$$

$$\frac{d\Omega}{dt} = \frac{1}{J} \iint_A [x_{sx} f_y - x_{sy} f_x] dA, \quad (12e)$$

(12) A: squirmer's surface,  $m$ : mass, and  $J$ : moment of inertia,  $\mathbf{f} = f_x \hat{\mathbf{e}}_x + f_y \hat{\mathbf{e}}_y$ : force density vector defined  $\forall x_s \in A$ ,

$$\mathbf{f}(x_s) = \boldsymbol{\tau}(x_s) \cdot \hat{\mathbf{n}}(x_s), \quad (13)$$

$\boldsymbol{\tau}(x_s)$  and  $\hat{\mathbf{n}}(x_s)$ : stress tensor and unit normal surface vector at  $x_s = x_{sx} \hat{\mathbf{e}}_x + x_{sy} \hat{\mathbf{e}}_y$ , respectively.

- Component-wise governing EOMs in the co-moving frame:

$$\frac{de_x}{dt} = -\Omega e_y, \quad \frac{de_y}{dt} = \Omega e_x, \quad (14a)$$

$$\frac{d\Omega}{dt} = \frac{1}{J} \iint_A [x_{sx} f_y - x_{sy} f_x] dA.$$

# Non-dimensionalisation

- Non-dimensional variables:

$$\tilde{x} = x/a, \quad \tilde{y} = t/a, \quad \tilde{x}_{sx} = x_{sx}/a, \quad \tilde{x}_{sy} = x_{sy}/a, \quad \tilde{t} = \frac{a}{U_s} t, \quad (15a)$$

$$\tilde{U}_x = U_x/U_s, \quad \tilde{U}_y = U_y/U_s, \quad \tilde{\Omega} = \frac{U_s}{a} \Omega, \quad (15b)$$

$$\tilde{f}_x = \frac{mU_s^2}{a} f_x, \quad \tilde{f}_y = \frac{mU_s^2}{a} f_y. \quad (15c)$$

- (15) ● Non-dimensional constants:

$$\tilde{x}_0 = x_0/a, \quad \tilde{y}_0 = y_0/a, \quad \tilde{L} = L/a. \quad (16)$$

- Non-dimensionalised EOMs in the lab frame:

$$\frac{d\tilde{x}}{d\tilde{t}} = \tilde{U}_x, \quad \frac{d\tilde{y}}{d\tilde{t}} = \tilde{U}_y, \quad (17a)$$

$$\frac{de_x}{d\tilde{t}} = -\tilde{\Omega}e_y, \quad \frac{de_y}{d\tilde{t}} = \tilde{\Omega}e_x, \quad (17b)$$

$$\frac{d\tilde{U}_x}{d\tilde{t}} = \iint_A \tilde{f}_x(x_s/a) dA, \quad (17c)$$

$$\frac{d\tilde{U}_y}{d\tilde{t}} = \iint_A \tilde{f}_y(x_s/a) dA, \quad (17d)$$

$$\frac{d\tilde{\Omega}}{d\tilde{t}} = 2 \iint_A [\tilde{x}_{sx}\tilde{f}_y - \tilde{x}_{sy}\tilde{f}_x] dA.$$

(17)



# Simulation parameters for the co-moving frame

- Domain size:  $50 \times 50$ ,
- IC and BCs (Eqn. (9)) are applied to the four sides.
- To solve the N-S equations (Eqn. (7)) using FEM, temporal resolutions are chosen as unity;  $\rho = Re_s = 0.01$  and  $\mu = 1$ .
- Single squirmer;  $a = 1$ ; initial position  $(\tilde{x}_0, \tilde{y}_0) = (25, 25)$ ; initial orientation  $\theta_0$ .
- Euler's method used to solve the non-dimensional governing EOMs (Eqn. (17)) on the steady-state flow fields; iterations continued until  $|U_s - B_1/2| \leq 0.001$ ; time step  $\Delta t = 1$ .
- Mesh elements: *free triangular*, mesh size near the squirmer's surface  $< 0.025$ , for the rest of the domain  $< 1$ .

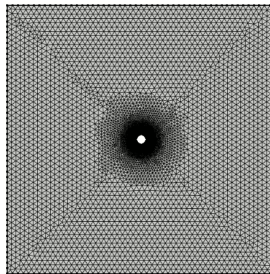
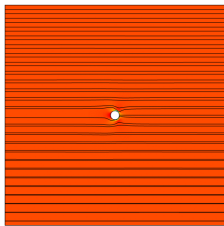


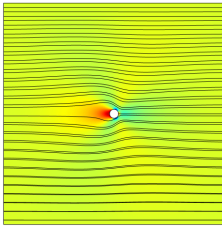
**Figure:** The simulation mesh employed in COMSOL for the co-moving frame has a maximum element size of 1 for the majority of the domain, with a smaller maximum size of 0.025 near the surface of the squirmer.



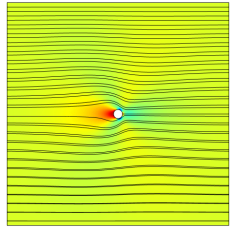
# Velocity profile



(a) Initial time



(b) Intermediate time



(c) Final time

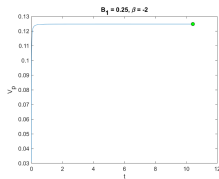


(d) Flow velocity magnitude scale

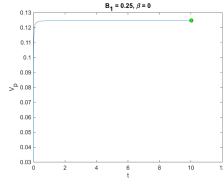
**Figure:** Temporal evolution of velocity fields induced by a puller with first swimming mode  $B_1 = 2$  and self-propulsion strength  $\beta = 2$  in an unbounded domain with quiescent fluid, as simulated using COMSOL. Black streamlines highlight propulsion mechanism at different time instances. Flow velocity magnitude scale is represented in (d).



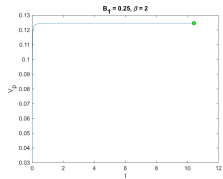
# Time evolution of the squirmer's velocity magnitude



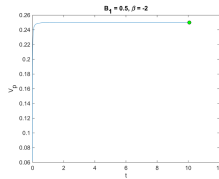
(a)  $B_1 = 0.25, \beta = -2$



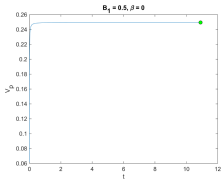
(b)  $B_1 = 0.25, \beta = 0$



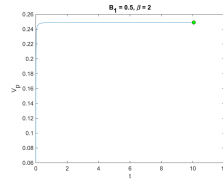
(c)  $B_1 = 0.25, \beta = 2$



(d)  $B_1 = 0.5, \beta = -2$



(e)  $B_1 = 0.5, \beta = 0$

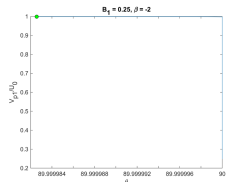


(f)  $B_1 = 0.5, \beta = 2$

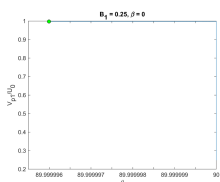
**Figure:** The non-dimensional velocity magnitude of the squirmer,  $\tilde{U}_s$ , as a function of non-dimensional time  $\tilde{t}$  for different values of  $B_1$  and  $\beta$ .



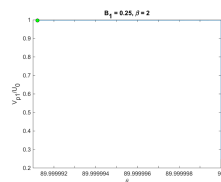
# Variation of the x-component of squirmer's velocity with orientation



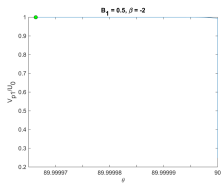
(a)  $B_1 = 0.25, \beta = -2$



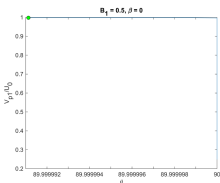
(b)  $B_1 = 0.25, \beta = 0$



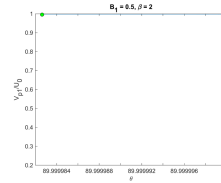
(c)  $B_1 = 0.25, \beta = 2$



(d)  $B_1 = 0.5, \beta = -2$



(e)  $B_1 = 0.5, \beta = 0$



(f)  $B_1 = 0.5, \beta = 2$

**Figure:** The behavior of the non-dimensional x-component of the squirmer's velocity,  $\tilde{U}_x$ , as a function of the orientational angle  $\theta$ , for various  $B_1$  and  $\beta$  values



# Variation of the $y$ -component of squirmer's velocity with orientation

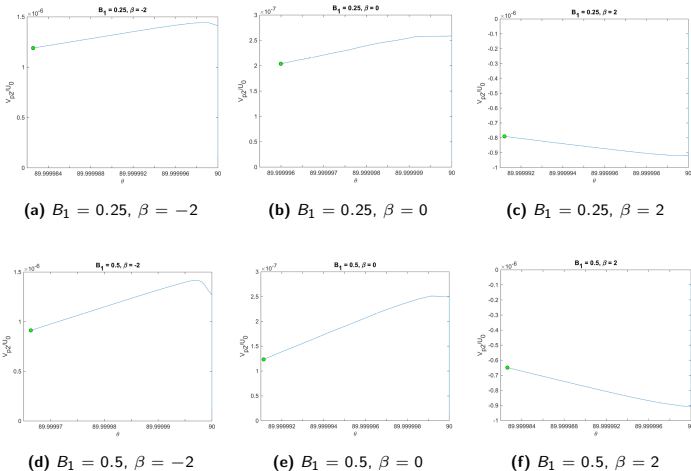


**Figure:** The  $y$ -component of the squirmer's non-dimensional velocity,  $\tilde{U}_y$ , is plotted against orientational angle  $\theta$  for different values of  $B_1$  and  $\beta$ .



# Variation of the squirmer's rotational speed with orientation

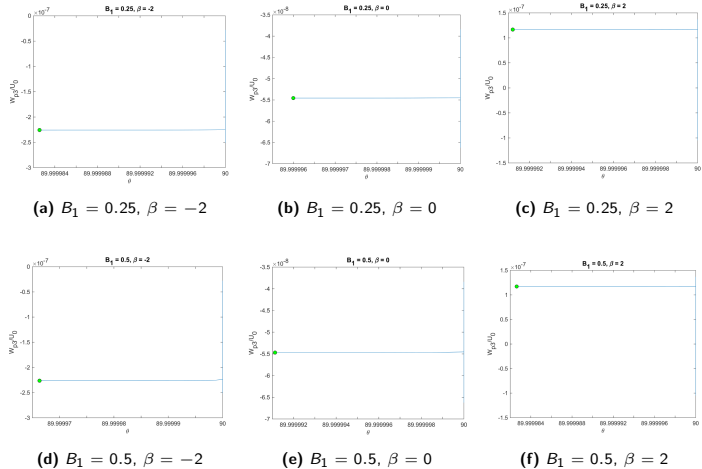


**Figure:** The non-dimensional rotational speed,  $\tilde{\Omega}$ , of the squirmer as a function of the orientational angle,  $\theta$ , for various values of  $B_1$  and  $\beta$ .

# Contents

- 1 Introduction
- 2 Swimming dynamics in unbounded quiescent fluid
  - Mathematical modelling
  - Numerical method
  - Results and discussion
- 3 Swimming dynamics in confined quiescent fluid
  - Mathematical modelling
  - Numerical method
  - Results and discussion



# Domain specifications in $x$ -moving frame

- **$x$ -moving frame:** A frame that translates with the  $x$ -component of the squirmer's velocity,  $U_x$ .
- A non-deformable 2D disk: radius  $a$ , initial position  $\mathbf{x}_0 = (x_0 = H, y_0 = 0)$ .
- Rectangular domain: length  $L = 16a$  or  $L = 20a$ , height  $H = L/2$ .
- Fluid: density  $\rho$ , dynamic viscosity  $\mu$ , Reynolds number  $Re_s$ .
- Horizontal centreline:  $y = 0$ ; top and bottom walls:  $y = \pm H/2$ , velocity  $-U_x \hat{\mathbf{e}}_x$ ; origin is located at the intersection of the horizontal centreline and the left boundary.

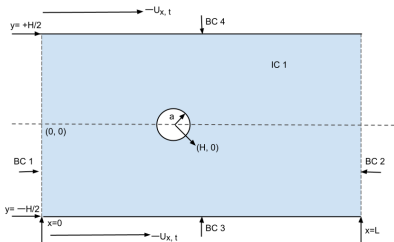


**Figure:** The figure illustrates the initial configuration of a rectangular microchannel in the  $x$ -moving frame, containing a stationary fluid and a squirmer of radius  $a$ . The rectangular domain has a length of either  $L = 16a$  or  $L = 20a$  and a height of  $H = L/2$ . The walls located at  $y = \pm H/2$  move with a velocity  $-U_x \hat{\mathbf{e}}_x$ . At the start of the simulation, the squirmer, a non-deformable two-dimensional disk with radius  $a$ , is positioned at  $\mathbf{x}_0 = (H, 0)$ . The initial and boundary conditions for the fluid velocity are described in Eqn. (19).

# Initial and boundary conditions in $x$ -moving frame

- Lab frame initial and boundary conditions:

$$\text{IC 1: } \mathbf{u}(x, y, t) = \mathbf{0} \text{ at } 0 \leq x \leq L, -\frac{H}{2} \leq y \leq \frac{H}{2}, t = 0, \quad (18\text{a})$$

$$\text{BC 1: } \mathbf{u}(x, y, t) = \mathbf{0} \text{ at } x = 0, -\frac{H}{2} \leq y \leq \frac{H}{2}, t \geq 0, \quad (18\text{b})$$

$$\text{BC 2: } \mathbf{u}(x, y, t) = \mathbf{0} \text{ at } x = L, -\frac{H}{2} \leq y \leq \frac{H}{2}, t \geq 0, \quad (18\text{c})$$

$$\text{BC 3 (no slip): } \mathbf{u}(x, y, t) = \mathbf{0} \text{ at } 0 \leq x \leq L, y = -\frac{H}{2}, t \geq 0, \quad (18\text{d})$$

$$\text{BC 4 (no slip): } \mathbf{u}(x, y, t) = \mathbf{0} \text{ at } 0 \leq x \leq L, y = \frac{H}{2}, t \geq 0. \quad (18\text{e})$$

- (18)   $x$ -moving frame initial and boundary conditions:

$$\text{IC 1: } \mathbf{u}(x, y, t) = -U_{x0}\hat{\mathbf{e}}_x \text{ at } 0 \leq x \leq L, -\frac{H}{2} \leq y \leq \frac{H}{2}, t = 0, \quad (19\text{a})$$

$$\text{BC 1: } \mathbf{u}(x, y, t) = -U_{x,t}\hat{\mathbf{e}}_x \text{ at } x = 0, -\frac{H}{2} \leq y \leq \frac{H}{2}, t \geq 0, \quad (19\text{b})$$

$$\text{BC 2: } \mathbf{u}(x, y, t) = -U_{x,t}\hat{\mathbf{e}}_x \text{ at } x = L, -\frac{H}{2} \leq y \leq \frac{H}{2}, t \geq 0, \quad (19\text{c})$$

$$\text{BC 3: } \mathbf{u}(x, y, t) = -U_{x,t}\hat{\mathbf{e}}_x \text{ at } 0 \leq x \leq L, y = -\frac{H}{2}, t \geq 0, \quad (19\text{d})$$

$$\text{BC 4: } \mathbf{u}(x, y, t) = -U_{x,t}\hat{\mathbf{e}}_x \text{ at } 0 \leq x \leq L, y = \frac{H}{2}, t \geq 0,$$

(19)  $U_{x0}$ :  $x$ -component of the squirmer velocity at  $t = 0$ ,  $U_{x,t}$ :  $x$ -component of the squirmer velocity at any time  $t$ .



# Squirmer dynamics: surface velocity

- Squirmer's position:  $\mathbf{x} = x\hat{\mathbf{e}}_x + y\hat{\mathbf{e}}_y$ ; orientation:  $\hat{\mathbf{e}} = e_x\hat{\mathbf{e}}_x + e_y\hat{\mathbf{e}}_y$ ;  
translational velocity:  $\mathbf{U}_s = U_x\hat{\mathbf{e}}_x + U_y\hat{\mathbf{e}}_y$ ; rotational velocity:  $\boldsymbol{\Omega} = \Omega\hat{\mathbf{e}}_z$ .

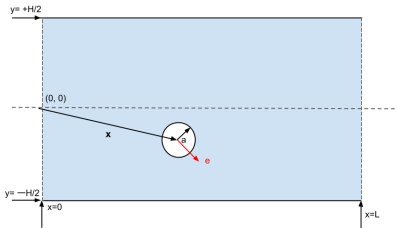


Figure: Schematic representation of the position and orientation of the squirmer in a rectangular microchannel.

- In the lab frame:

$$\begin{aligned}\mathbf{u}_s(\mathbf{x}_s) &= \mathbf{u}^S(\mathbf{x}_s) + \mathbf{U}_s + \boldsymbol{\Omega} \times \mathbf{x}_s \\ &= B_1 (\sin \theta + 2\beta \sin \theta \cos \theta) \hat{\mathbf{e}}_\theta + \mathbf{U}_s + \boldsymbol{\Omega} \times \mathbf{x}_s.\end{aligned}\tag{20}$$

- In the  $x$ -moving frame:

$$\begin{aligned}\mathbf{u}_s(\mathbf{x}_s) &= \mathbf{u}^S(\mathbf{x}_s) + U_y\hat{\mathbf{e}}_y + \boldsymbol{\Omega} \times \mathbf{x}_s \\ &= B_1 (\sin \theta + 2\beta \sin \theta \cos \theta) \hat{\mathbf{e}}_\theta + U_y\hat{\mathbf{e}}_y + \boldsymbol{\Omega} \times \mathbf{x}_s.\end{aligned}$$



# Squirmer dynamics: governing EOMs

- Component-wise governing EOMs in the lab frame:

$$\frac{dx}{dt} = U_x, \quad \frac{dy}{dt} = U_y, \quad (22a)$$

$$\frac{de_x}{dt} = -\Omega e_y, \quad \frac{de_y}{dt} = \Omega e_x, \quad (22b)$$

$$\frac{dU_x}{dt} = \frac{1}{m} \iint_A f_x(\mathbf{x}_s) dA, \quad (22c)$$

$$\frac{dU_y}{dt} = \frac{1}{m} \iint_A f_y(\mathbf{x}_s) dA, \quad (22d)$$

$$\frac{d\Omega}{dt} = \frac{1}{J} \iint_A [x_{sx} f_y - x_{sy} f_x] dA, \quad (22e)$$

(22) A: squirmer's surface,  $m$ : mass, and  $J$ : moment of inertia,  $\mathbf{f} = f_x \hat{\mathbf{e}}_x + f_y \hat{\mathbf{e}}_y$ : force density vector defined  $\forall \mathbf{x}_s \in A$ ,

$$\mathbf{f}(\mathbf{x}_s) = \boldsymbol{\tau}(\mathbf{x}_s) \cdot \hat{\mathbf{n}}(\mathbf{x}_s), \quad (23)$$

$\boldsymbol{\tau}(\mathbf{x}_s)$  and  $\hat{\mathbf{n}}(\mathbf{x}_s)$ : stress tensor and unit normal surface vector at  $\mathbf{x}_s = x_{sx} \hat{\mathbf{e}}_x + x_{sy} \hat{\mathbf{e}}_y$ , respectively.

- Component-wise governing EOMs in the  $x$ -moving frame:

$$\frac{dy}{dt} = U_y, \quad (24a)$$

$$\frac{de_x}{dt} = -\Omega e_y, \quad \frac{de_y}{dt} = \Omega e_x, \quad (24b)$$

$$\frac{dU_y}{dt} = \frac{1}{m} \iint_A f_y(\mathbf{x}_s) dA, \quad (24c)$$

$$\frac{d\Omega}{dt} = \frac{1}{J} \iint_A [x_{sx} f_y - x_{sy} f_x] dA. \quad (24d)$$

# Non-dimensionalisation

- Non-dimensional variables:

$$\tilde{x} = x/a, \quad \tilde{y} = t/a, \quad \tilde{x}_{sx} = x_{sx}/a, \quad \tilde{x}_{sy} = x_{sy}/a, \quad \tilde{t} = \frac{a}{U_s} t, \quad (25a)$$

$$\tilde{U}_x = U_x/U_s, \quad \tilde{U}_y = U_y/U_s, \quad \tilde{\Omega} = \frac{U_s}{a} \Omega, \quad (25b)$$

$$\tilde{f}_x = \frac{mU_s^2}{a} f_x, \quad \tilde{f}_y = \frac{mU_s^2}{a} f_y. \quad (25c)$$

(25)

- Non-dimensional constants:

$$\tilde{x}_0 = x_0/a, \quad \tilde{y}_0 = y_0/a, \quad \tilde{L} = L/a, \quad \tilde{H} = H/a. \quad (26)$$

- Non-dimensionalised EOMs in the  $x$ -moving frame:

$$\frac{d\tilde{y}}{d\tilde{t}} = \tilde{U}_y, \quad (27a)$$

$$\frac{de_x}{d\tilde{t}} = -\tilde{\Omega}e_y, \quad \frac{de_y}{d\tilde{t}} = \tilde{\Omega}e_x, \quad (27b)$$

$$\frac{d\tilde{U}_y}{d\tilde{t}} = \iint_A \tilde{f}_y(x_s/a) dA, \quad (27c)$$

$$\frac{d\tilde{\Omega}}{d\tilde{t}} = 2 \iint_A \left[ \tilde{x}_{sx} \tilde{f}_y - \tilde{x}_{sy} \tilde{f}_x \right] dA. \quad (27d)$$

(27)

# Wall-induced interactions

- Wall-induced hydrodynamic interactions:

$$\frac{d\tilde{x}}{d\tilde{t}} = \frac{1}{2}(1 - \lambda^2) [-B_1 \sin \theta + 2\lambda B_2 \sin(2\theta)], \quad (28a)$$

$$\frac{d\tilde{y}}{d\tilde{t}} = \frac{(1 - \lambda^2)^2}{2(1 + \lambda^2)} [B_1 \cos \theta + 2\lambda B_2 \sin(2\theta)], \quad (28b)$$

$$\frac{d\hat{\mathbf{e}}_x}{d\tilde{t}} = \frac{\lambda^2}{1 + \lambda^2} [2\lambda B_1 \sin \theta - (1 - 3\lambda^2) B_2 \cos(2\theta)] \sin \theta, \quad (28c)$$

$$\frac{d\hat{\mathbf{e}}_y}{d\tilde{t}} = \frac{\lambda^2}{1 + \lambda^2} [-2\lambda B_1 \sin \theta + (1 - 3\lambda^2) B_2 \cos(2\theta)] \cos \theta, \quad (28d)$$

$\lambda = \tilde{h} - (\tilde{h}^2 - 1)^{1/2}$ ,  $\tilde{h} = \frac{\tilde{H}}{2} - |\tilde{y}|$ : distance of the squirmer's centre from the nearer wall.

- Wall-induced non-hydrodynamic repulsion force:

$$\mathbf{F}_{rep} = -F_{rep}\hat{\mathbf{e}}_y = -\frac{Ae^{-Bd}}{1 - e^{-Bd}}\hat{\mathbf{e}}_y, \quad (29)$$

$d = \left| \frac{\tilde{H}}{2} - \tilde{x}_y - 1 \right|$ : minimum distance between the body surface of the squirmer and the nearest wall.



# Modified EOMs incorporating non-hydrodynamic interactions

Modified non-dimensionalised EOMs in the  $x$ -moving frame:

$$\frac{d\tilde{y}}{d\tilde{t}} = \tilde{U}_y, \quad (30a)$$

$$\frac{de_x}{d\tilde{t}} = -\tilde{\Omega}e_y, \quad \frac{de_y}{d\tilde{t}} = \tilde{\Omega}e_x, \quad (30b)$$

$$\frac{d\tilde{U}_y}{d\tilde{t}} = \iint_A \tilde{f}_y(x_s/a) dA - F_{rep}. \quad (30c)$$

$$\frac{d\tilde{\Omega}}{d\tilde{t}} = 2 \iint_A [\tilde{x}_{sx} \tilde{f}_y - \tilde{x}_{sy} \tilde{f}_x] dA. \quad (30d)$$

(30)

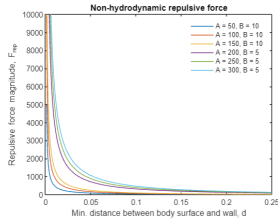


**Figure:** Plot showing the variation of the magnitude of the non-hydrodynamic repulsive force, denoted by  $F_{rep}$ , as a function of the minimum distance  $d$  between the surface of the squirmer's body and the nearest wall, for different combinations of the parameters  $A$  and  $B$ .

# Simulation parameters for the x-moving frame

- Domain size:  $8 \times 16$  or  $10 \times 20$ .
- IC and BCs in Eqn. (19) are imposed on the bottom and top walls, and the remaining two sides.
- To solve the N-S equations (Eqn. (7)) using FEM, temporal resolutions are chosen as unity;  $\rho = Re_s = 0.01$  and  $\mu = 1$ .
- Single squirmer;  $a = 1$ ; initial position  $(\tilde{x}_0, \tilde{y}_0) = (8, 0)$ ; initial orientation  $\theta_0$ .
- Euler's method used to solve the non-dimensional governing EOMs (Eqns. (17), (27), (30)) on the steady-state flow fields; iterations continued until a puller with  $B_1 = 2$  and  $\beta = 1$  reaches a steady-state value of velocity magnitude, or until a time of  $10^3$  is reached; time step  $\Delta t = 1$ .
- Mesh elements: *free triangular*, mesh size near the squirmer's surface, as well as the top and bottom walls  $< 0.025$ , for the rest of the domain  $< 1$ .
- Additionally, for vertical squirmer motion: *deformed mesh feature* enabled; for accurate simulations, *automatic remeshing* enabled.

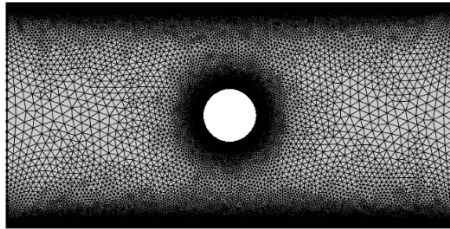
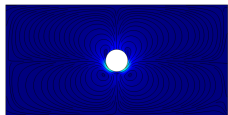


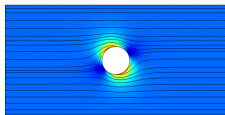
**Figure:** Mesh used in the simulations in the co-moving frame, with maximum element size of 1 for the majority of the domain and 0.02 near the squirmer's surface and top/bottom walls. The mesh is shown for a simulation domain of  $8 \times 16$ .



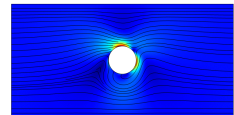
# Velocity profile



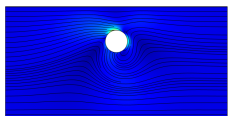
(a) Pusher, initial time



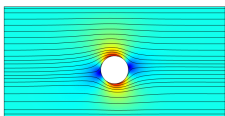
(b) Neutral, initial time



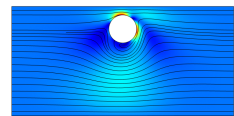
(c) Puller, initial time



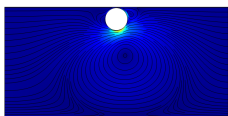
(d) Pusher, halfway point



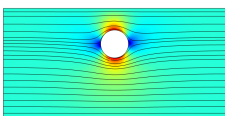
(e) Neutral, halfway point



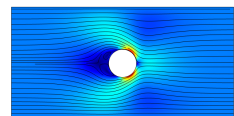
(f) Puller, halfway point



(g) Pusher, final time



(h) Neutral, final time

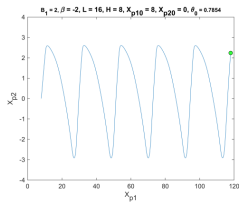


(i) Puller, final time

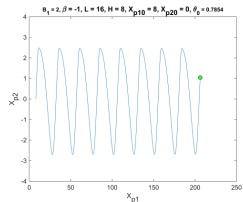


(j) Flow velocity magnitude scale

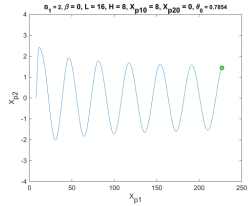
# Confinement-induced trajectories



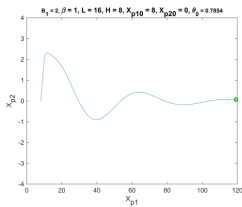
(a)  $B_1 = 2, \beta = -2, \theta_0 = \pi/4$



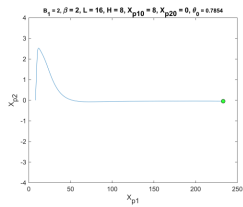
(b)  $B_1 = 2, \beta = -1, \theta_0 = \pi/4$



(c)  $B_1 = 2, \beta = 0, \theta_0 = \pi/4$



(d)  $B_1 = 2, \beta = 1, \theta_0 = \pi/4$



(e)  $B_1 = 2, \beta = 2, \theta_0 = \pi/4$

**Figure:** Trajectories of squirmers with  $B_1 = 2$  and varying  $\beta$  values in a rectangular microchannel with quiescent fluid. Squirmers with negative  $\beta$  values are pushers while those with positive  $\beta$  values are pullers. The initial condition for all trajectories is  $(\bar{x}, \bar{y}, \theta) = (H, 0, \pi/4)$ .



# Time evolution of the squirmer's velocity magnitude

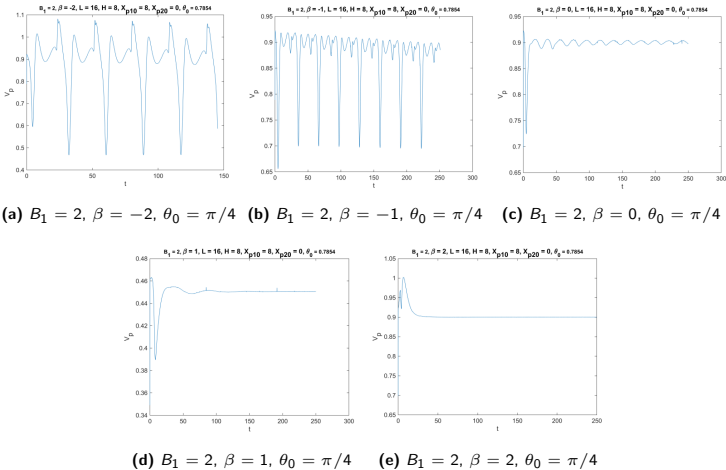
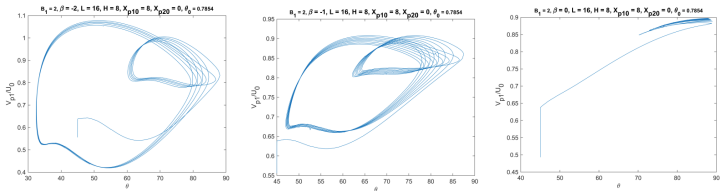
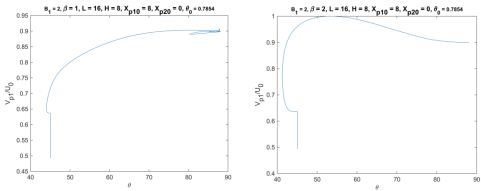


**Figure:** The figure illustrates the temporal evolution of the magnitude of velocity  $U_p$  for squirmers with first swimming mode  $B_1 = 2$  and varying self-propulsion strengths  $\beta$  in a rectangular microchannel with quiescent fluid. The plots are initialized with  $(\tilde{x}, \tilde{y}, \theta) = (H, 0, \pi/4)$  for all cases. The figure shows that squirmers with different values of  $\beta$  exhibit distinct oscillatory behaviors with time, and the rate of decay in the amplitude of the oscillations depends on the type of squirmer and the value of  $\beta$ .

# Variation of the x-component of squirmer's velocity with orientation



**(a)  $B_1 = 2, \beta = -2, \theta_0 = \pi/4$  (b)  $B_1 = 2, \beta = -1, \theta_0 = \pi/4$  (c)  $B_1 = 2, \beta = 0, \theta_0 = \pi/4$**

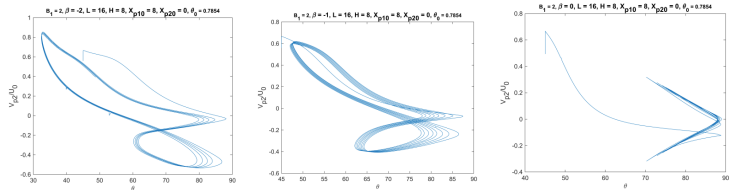


**(d)  $B_1 = 2, \beta = 1, \theta_0 = \pi/4$  (e)  $B_1 = 2, \beta = 2, \theta_0 = \pi/4$**

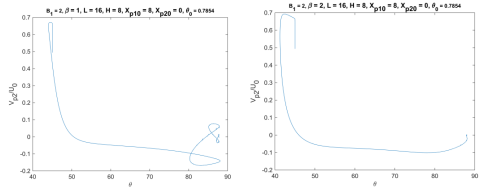
**Figure:** x-component of the velocity,  $U_x$ , of squirmers with first swimming mode  $B_1 = 2$  and different self-propulsion strengths  $\beta$  as a function of orientation angle  $\theta$  in a rectangular microchannel with quiescent fluid. The initial condition for all plots is  $(\tilde{x}, \tilde{y}, \theta) = (H, 0, \pi/4)$ .



# Variation of the $y$ -component of squirmer's velocity with orientation



(a)  $B_1 = 2, \beta = -2, \theta_0 = \pi/4$  (b)  $B_1 = 2, \beta = -1, \theta_0 = \pi/4$  (c)  $B_1 = 2, \beta = 0, \theta_0 = \pi/4$



(d)  $B_1 = 2, \beta = 1, \theta_0 = \pi/4$  (e)  $B_1 = 2, \beta = 2, \theta_0 = \pi/4$

**Figure:**  $y$ -component of the velocity,  $U_y$ , of squirmers with first swimming mode  $B_1 = 2$  and different self-propulsion strengths  $\beta$  as a function of orientation angle  $\theta$  in a rectangular microchannel with quiescent fluid. The initial condition for all plots is  $(\tilde{x}, \tilde{y}, \tilde{\theta}) = (H, 0, \pi/4)$ .



# References

- [1] P Ahana and Sumesh P Thampi. Confinement induced trajectory of a squirmer in a two dimensional channel. *Fluid Dynamics Research*, 51(6):065504, 2019.
- [2] Michael J Lighthill. On the squirming motion of nearly spherical deformable bodies through liquids at very small reynolds numbers. *Communications on pure and applied mathematics*, 5(2):109–118, 1952.
- [3] JR Blake. Self propulsion due to oscillations on the surface of a cylinder at low reynolds number. *Bulletin of the Australian Mathematical Society*, 5(2):255–264, 1971.
- [4] Donald L Koch and Ganesh Subramanian. Collective hydrodynamics of swimming microorganisms: living fluids. *Annual Review of Fluid Mechanics*, 43:637–659, 2011.
- [5] Saverio E Spagnolie and Eric Lauga. Hydrodynamics of self-propulsion near a boundary: predictions and accuracy of far-field approximations. *Journal of Fluid Mechanics*, 700:105–147, 2012.
- [6] Ye Li, He Zhai, Sandra Sanchez, Daniel B Kearns, and Yilin Wu. Noncontact cohesive swimming of bacteria in two-dimensional liquid films. *Physical review letters*, 119(1):018101, 2017.
- [7] Henry Shum and Eamonn A Gaffney. Hydrodynamic analysis of flagellated bacteria swimming near one and between two no-slip plane boundaries. *Physical Review E*, 91(3):033012, 2015.
- [8] Federico Fadda, John Jairo Molina, and Ryoichi Yamamoto. Dynamics of a chiral swimmer sedimenting on a flat plate. *Physical Review E*, 101(5):052608, 2020.
- [9] Nicholas C Darnton, Linda Turner, Svetlana Rojevsky, and Howard C Berg. Dynamics of bacterial swarming. *Biophysical journal*, 98(10):2082–2090, 2010.
- [10] Eric Lauga, Willow R DiLuzio, George M Whitesides, and Howard A Stone. Swimming in circles: motion of bacteria near solid boundaries. *Biophysical journal*, 90(2):400–412, 2006.
- [11] Deming Nie, Yuxiang Ying, Geng Guan, Jianzhong Lin, and Zhenyu Ouyang. Two-dimensional study on the motion and interactions of squirmers under gravity in a vertical channel. *Journal of Fluid Mechanics*, 960:A31, 2023.
- [12] Jeffrey A Riffell and Richard K Zimmer. Sex and flow: the consequences of fluid shear for sperm–egg interactions. *Journal of Experimental Biology*, 210(20):3644–3660, 2007.
- [13] Stefano Fusco, George Chatzipiridis, Kartik M Sivaraman, Olgaç Ergeneman, Bradley J Nelson, and Salvador Pané. Chitosan electrodeposition for microrobotic drug delivery. *Advanced healthcare materials*, 2(7):1037–1044, 2013.
- [14] Jens Elgeti, Roland G Winkler, and Gerhard Gompper. Physics of microswimmers—single particle motion and collective behavior: a review. *Reports on progress in physics*, 78(5):056601, 2015.
- [15] Nicholas G Chisholm, Dominique Legendre, Eric Lauga, and Aditya S Khair. A squirmer across reynolds numbers. *Journal of Fluid Mechanics*, 796:233–256, 2016.
- [16] On Shun Pak and Eric Lauga. Generalized squirming motion of a sphere. *Journal of Engineering Mathematics*, 88:1–28, 2014.

